Open Access

Journal of Energy and Power Technology

LIDSEN Publishing Inc.

Original Research

A Comparative Study of R134a and Propane (R290) as Refrigerants in Heat Pump Water Heaters

Ann Lee *, Shaokoon Cheng

School of Engineering, Macquarie University, NSW 2109, Australia; E-Mails: ann.lee@mq.edu.au; shaokoon.cheng@mq.edu.au

* **Correspondence:** Ann Lee; E-Mail: ann.lee@mq.edu.au

Academic Editor: Xiaolin Wang

Special Issue: Decarbonisation of Heating and Cooling

Journal of Energy and Power Technology
2023, volume 5, issue 3
doi:10.21926/jept.2303029

Received: March 26, 2023
Accepted: September 12, 2023
Published: September 18, 2023

Abstract

In the context of decarbonization efforts, heat pump water heaters (HPWHs) offer an attractive solution over conventional electric resistance type hot water systems due to their 2-3 times higher efficiency. However, the high manufacturing costs and taxes associated with using hydrofluorocarbon (HFC) refrigerant make HPWHs expensive. As a means to tackle this issue, this paper explores the use of propane (R290) as a refrigerant in HPWHs. The study involves an experimental comparison of R290 and R134a, with refrigerant charges optimized for the unit at different ambient temperatures. This current work demonstrates that R290 achieves a 10% improvement in coefficient of performance (COP) at ambient temperatures beyond 20°C. However, at 10°C ambient temperature, the study shows that R290 offers no advantage over R134a, and the COP is lower. These results indicate that the compressor is the largest source of inefficiency, and this aligns well with experimental results on system performance. Additionally, simulation tests using compressors designed for R290 did not predict better COP values than the test unit. Overall, the study suggests that R290 is a viable refrigerant option for HPWHs, but further research is necessary to optimize it's use.

Keywords
Heat pump water heater; propane (R290); R134a; refrigerant

1. Introduction

In the last two decades, HPWHs have drawn considerable attention as one type of hot water system due to their high efficiency, making them an important tool for decarbonisation efforts. Compared to traditional electric resistance-based hot water systems, HPWHs can improve efficiency by 2-3 times, leading to lower operating costs [1]. Although government incentives in several countries have helped promote the use of HPWHs, their adoption is limited due to the exorbitant upfront cost of manufacturing these products. One challenge of using HPWHs is using alternative refrigerants that are environmentally friendly but do not come with the caveat of higher cost. The standard refrigerant class typically found in domestic HPWHs, Hydrofluorocarbons (HFCs), is inexpensive but has been known to trap several hundred times the amount of heat in the atmosphere more than carbon dioxide, making their replacement critical for achieving decarbonisation goals. Not surprisingly, HFC, commonly known as R134a, has a GWP (global warming potential) rating of 1300 [2] and incurs three times the tax cost in Australia compared to other HFCs when used.

For the above reasons, The Montreal Protocol implemented regulations to phase out the use of HCFCs, including HFC refrigerants, progressively for the above reasons. In Australia, the use of HCFCs has been discouraged since 2016, and the import of HFCs has declined since the beginning of 2018 [3]. Propane, also known as R290, is a flammable natural refrigerant in the Halocarbon family of gases that is a viable alternative to HCFCs. However, propane was not initially considered an ideal refrigerant due to its flammable properties [4, 5]. Compared to HFCs, propane has a GWP of 3 and an ODP of 0 [6], suggesting that they are much less environmentally harmful.

When propane is used as a refrigerant, regulations must ensure that the amount of refrigerant charge in a given HPWH system is low and precautions to reduce leakage-related risks are warranted. This is an important measure to reduce the risk of catastrophic events, such as the well-known incident in Tamahere, New Zealand [7], which was caused by leakage in an HPWH with a hydrocarbon refrigerant consisting of 85% propane. It has been recommended that if a similar system is to be implemented, the refrigerant should have a stanching agent to warn of potential leaks [8]. The Australian Institute of Refrigeration, Air Conditioning, and Heating (AIRAH) recommend using a maximum of 150 g of R290 charge in small refrigeration systems [9], which is in line with the International Electrotechnical Commission's (IEC) safety standards [10]. However, this limits the use of R290 to small HPWH systems. Using R290 in larger systems would require a comprehensive risk assessment and third-party certification of safe operation [10].

The efficiency of Propane as a refrigerant has been demonstrated in many studies. For example, Devotta et al. [11] showed that the coefficient of performance of Propane was superior when used as a drop-in substitute for R22 in a window air conditioner. A theoretical study conducted by Maclaine-cross and Leonardi [12] identified R290 as having superior heat transfer properties to R134a. The liquid's thermal conductivity ratio to its dynamic viscosity (k/μ) at -15°C saturated liquid state is almost three times higher when R290 was used (0.785 kJ/kgK compared with 0.289

kJ/kgK). This parameter indicates that there is likely heat transfer associated forced convection in the condenser and evaporator. Furthermore, Danfoss[13] identified very similar critical temperatures, 96.7°C for R290, compared with 101°C for R134a, for the same latent heat transfer. Volumetric capacity for R290 is also 78% higher than R134a (1164 kJ/kg compared with 658 kJ/kg), indicating higher energy density with consequences of lower refrigerant charges being required for the same performance. The general consensus is that the only factor deterring the extensive use of R290 is its high flammability.

Gonzalvez et al. [14, 15] emphasized the importance of optimizing minimum charge hydrocarbon units for R290 as an approach to encourage their use. The minimization of charge has been made possible using specialized mini-channel aluminium heat exchangers, as successfully demonstrated by Granryd et al. [16] in previous work, where the charge was considerably reduced while maintaining the same coefficient of performance (COP). In addition to minimizing charge hydrocarbon units, performing exergy analysis is also significant for any thermodynamic system as it indicates the extent of energy loss in a system. Simply put, the exergy of a given system at a certain thermodynamic condition is the maximum amount of work that could be attained when the system moves from the specific state to the state of equilibrium with the surrounding [17]. Therefore, determining the exergy of a system can help define appropriate means to reduce energy losses and produce more efficient and effective energy systems. The benefits of performing exergy analysis were identified experimentally by Ahamed et al. [18], who suggested that the performance of individual components could be assessed by analyzing the change in exergy, which would otherwise be difficult to achieve through conventional COP analysis. Full mathematical formulations for exergy analysis in different components are presented in [18]. Despite the plethora of literature on the effects of evaporating temperature on exergy losses associated with different refrigerants and components, few existing works on exergy studies provide recommendations on how to improve thermodynamic systems [19, 20].

This paper explores the potential of R290 as a refrigerant in heat pump water heaters, evaluating its feasibility at different charges of 230 g, 260 g, and 290 g. In order to ensure safety, the study discusses safety measures in the experimental setup and adheres to the recommended safety charge for R290. Experimental tests were conducted at ambient temperatures ranging from 10°C to 30°C with an increment step of 5°C. A parallel experiment was also conducted to compare the performance of R290 with the benchmark case of R134a as a refrigerant in heat pump water heaters. Part of the result is compared to the literature [21] where an experimental study of an air-to-water reversible heat pump unit was conducted using R290. The simulation studies used the same settings as the experimental setup and exergy analysis was performed to assess the exergy destruction in each core component of the heat pump water heater. The current study utilized the flexible IMST-ART software to model compressors and different types of heat exchangers. The findings of this study provide valuable insights into the feasibility of R290 as a refrigerant and its potential to improve the performance of heat pump water heaters.

2. Experimental Setup

2.1 Experimental Setup

The experimental setup involved modifying an existing production model HDi-310 HPWH [22] by reducing the compressor capacity for safety purposes. To prevent ignition risk, the electronic controller was installed inside a sealed external enclosure (refer to Figure 1).

Figure 1 Controller unit mounted inside an enclosure to avoid an ignition source.

Safety switches were installed to shut down the system in the event of high or low pressure, as both situations can cause damage or indicate a leak in the system. In addition, hydrocarbon and oxygen gas sensors were designed and installed in the climate-controlled testing facility to shut down all power if tripped. The test unit was equipped with 11 thermocouples and two transducers to measure temperature and pressure at various locations throughout the system, as shown in Figure 2. Full details of the experimental setups for the compressor, condenser, evaporator, and thermal expansion valve are provided in Table 1, Table 2, Table 3, and Table 4, respectively. These tables present a thorough overview of the specifications and dimensions of each component, allowing for a comprehensive understanding of the experimental test system.

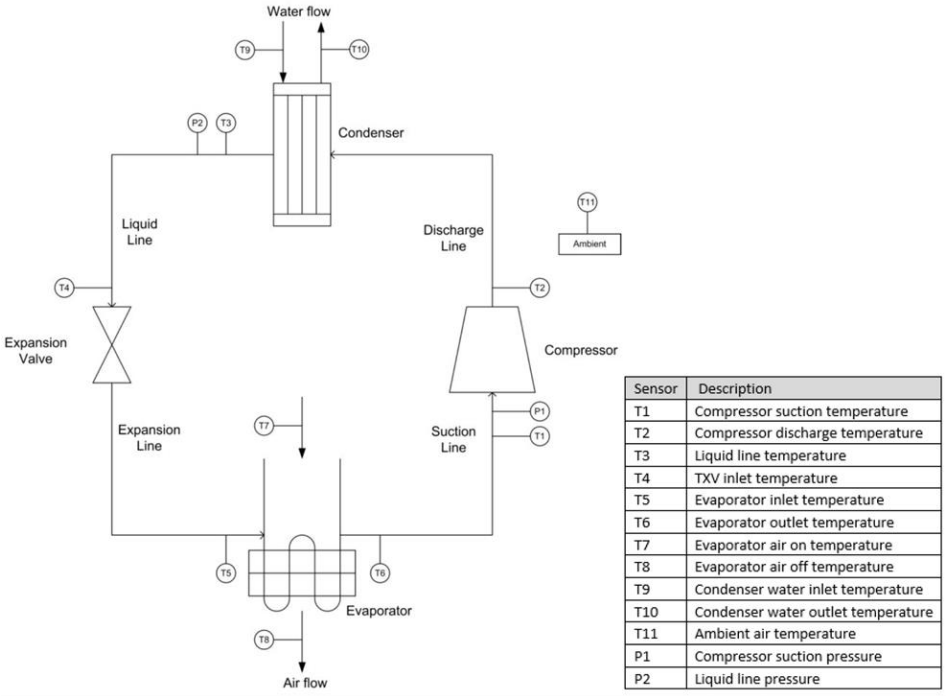

Sensor	Description
T1	Compressor suction temperature
T2	Compressor discharge temperature
T3	Liquid line temperature
T4	TXV inlet temperature
T5	Evaporator inlet temperature
T6	Evaporator outlet temperature
T7	Evaporator air on temperature
T8	Evaporator air off temperature
T9	Condenser water inlet temperature
T10	Condenser water outlet temperature
T11	Ambient air temperature
P1	Compressor suction pressure
P2	Liquid line pressure

Figure 2 Locations of thermocouples (T) and pressure transducers (P) on the system.

Table 1 Compressor specifications.

Displacement	13.5 cm^3/rev
Evaporating Pressure Range	0.26 ~ 0.73 MPa (-10 ~ +15°C)
Condensing Pressure Range	1.10 ~ 2.83 MPa (28 ~ 65°C)
Compression Ratio	≤6
Discharge Gas Temperature	Must not exceed 115°C
Motor Type	Single Phase Induction Motor
Rated Voltage	220-240 ± 10%
Rated Frequency	50 Hz ± 2%
ON/OFF cycle	ON/OFF cycle maximum 10 times an hour.
Amount of refrigerant charged	Maximum of 0.9 kg
Nominal Output	650 W
Nominal Revolution	2840/2860 RPM

Table 2 Condenser specifications.

Condenser Type	Counter flow brazed plate
Dimensions	377 × 119.5 × 36
Number of Plates	12
Plate material in contact with fluid	AISI 316 Stainless steel
Plate material not in contact with fluid	AISI 304 Stainless steel
Brazing Material	Pure copper
Standard connection material	AISI 316 Stainless steel

Max working pressure	**At 155°C**	31 bar
	At 225°C	27 bar
Temperature Range	**Min**	-196°C
	Max	225°C

Table 3 Evaporator specifications.

Fin Dimensions (H x L x W)	419.1 × 510 × 66 mm
Number of tube rows in airflow direction	3
Number of equivalent parallel circuits	16 (counted)
Type of fin surface	Wavy
Fin Pitch	2 mm
Fins Per Inch (FPI)	12
Fin Thickness	0.115 mm
Fin material	Aluminium
Tube material	Copper
Tube Construction	Plain tube

Table 4 Thermal expansion valve specifications.

Orifice Type		Fixed
Equalisation		Internal
Max working pressure		34 bar
Temperature range		-40 to 10°C
Material	**Element**	Stainless steel
	Valve Body	Brass
	Bulb and capillary tube	Copper

2.2 Charge Determination

Charge determination was carried out to determine the optimal amount of refrigerant needed to fill the system. 50 L of water in a tank was heated, and ball valves were installed at the outlet drain and inlet controlled water. Charge determination was performed under high ambient temperatures of 40°C and low ambient temperatures of 10°C. A single charge was tested for three tank water temperatures of 15°C, 20°C, and 30°C, resulting in six conditions being tested for a single charge. The evaporator superheat, and condenser sub-cool values were primarily monitored for each condition. This process was repeated for charges ranging from 400 to 900 g of R134a with approximately 30 g of incremental charge. Figure 3(a) and (b) depict charge determination for a high ambient temperature of 40°C and a low ambient temperature of 10°C, respectively. The superheated temperature, sub-cooled temperature, and liquid line pressure were plotted at several charges for both cases. Based on minimal superheat in the low ambient condition and reduced liquid line pressure, a charge of 700 g R134a was selected. Due to the low density of R290, direct charge determination using this refrigerant was deemed impractical. Instead, the optimal charge for R290 was estimated indirectly by first determining the optimal charge for R134a.

Subsequently, the optimal charge for R290 was estimated by scaling based on refrigerant densities, following the recommendation provided by the refrigerant supplier.

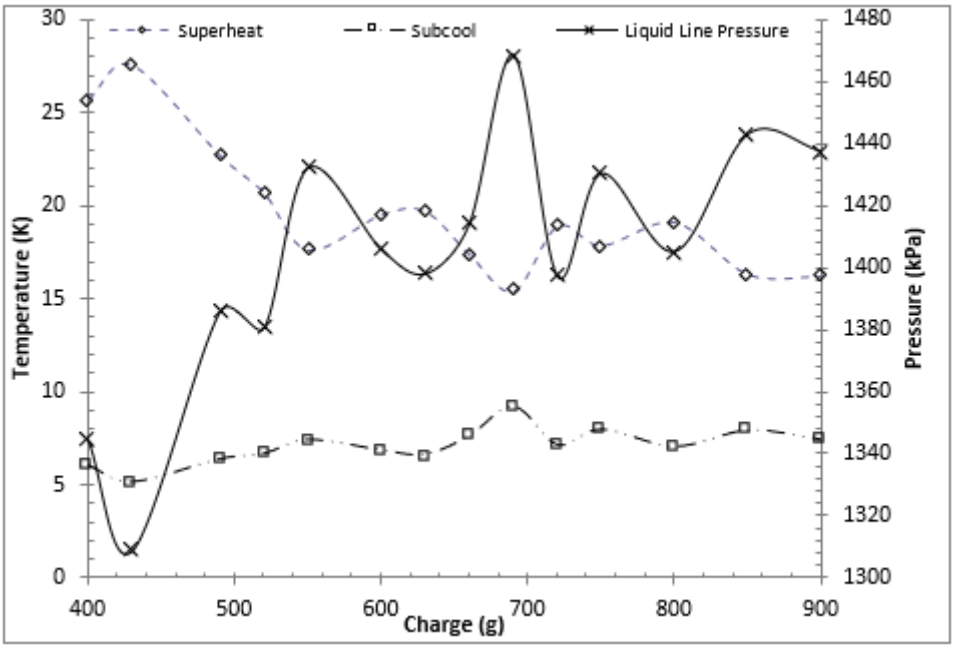

(a)

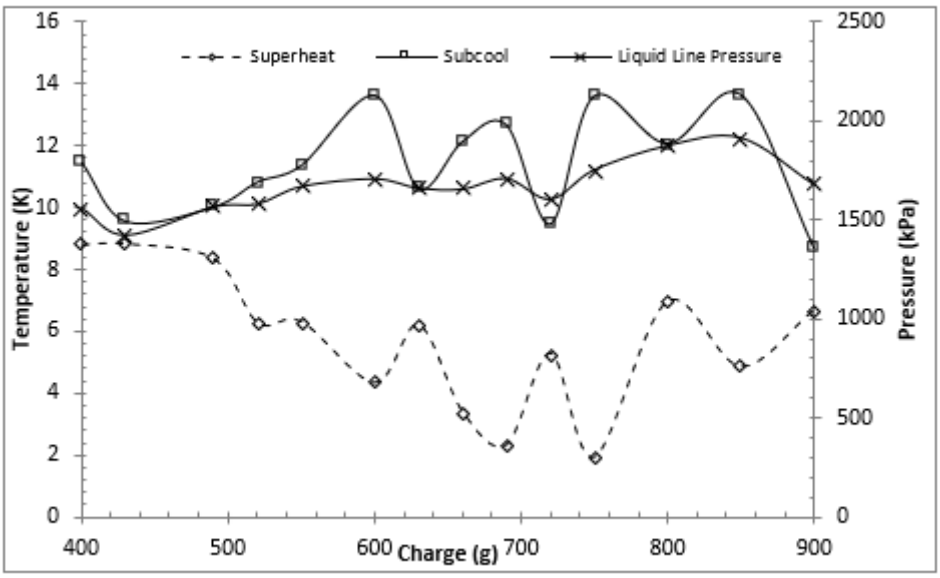

(b)

Figure 3 Charge determination at ambient temperature (a) 40°C ambient, 15°C Water condition, (b) 10°C ambient, 30°C Water condition.

2.3 Performance Testing

Two additional changes were implemented on the test unit before the testing commenced. Firstly, two filter sheets were added on the evaporator air sides to decrease the high superheat of 15 K to 6.1 K at 30°C ambient conditions. Secondly, an insulation jacket was fitted around the

compressor, as shown in Figure 4. Additionally, the 310 L tank was reconnected, and six tank sensors were installed to measure the water temperature at different levels of the tank.

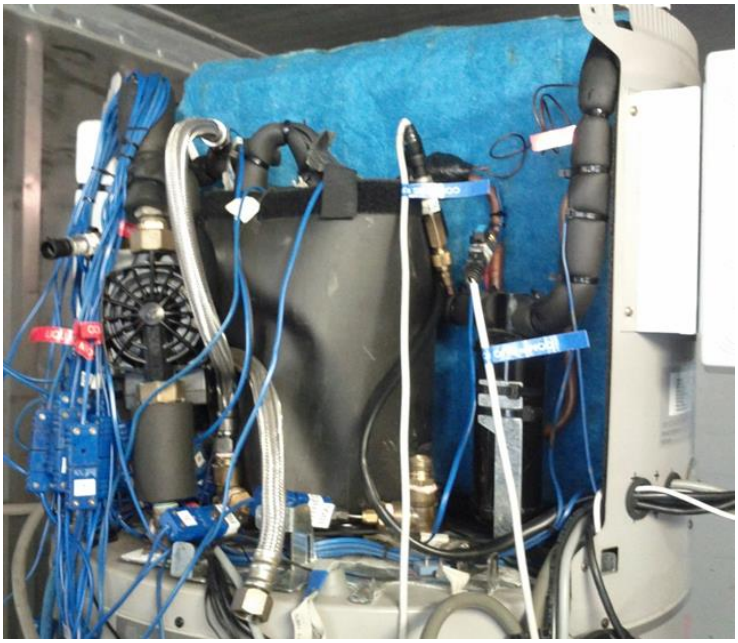

Figure 4 Test unit with insulation jacket around compressor and two filter sheets on the evaporator.

The test procedure for conducting full heat-up cycle tests at the varying ambient air temperature was as follows:

1. The controlled room was set to a specific ambient air temperature (10°C, 15°C, 20°C, 25°C, 30°C), and allowed to stabilize.
2. The 310 L tank was filled with mains water so that the initial temperature of the water recorded by all six tank sensors was 20°C, and the room was locked to prevent any disturbance during the test.
3. The DT80 data logger was remotely initialized via an outside computer, so all thermocouples and pressure transducers were being recorded.
4. The heat pump was switched on remotely.
5. The test was allowed to run until the electronic controller detected a full heat-up cycle and switched off automatically. Typically, this was when the top four tank sensors reached 60°C, and the bottom-most tank sensor reached 50°C.
6. The DT80 data logger was then stopped, and data were extracted before its memory was cleared for the next test.

3. Theory and Simulation

3.1 Energy Analysis

The calculation for Coefficient of Performance (COP) was based on the general definition,

$$COP = \frac{Q_{out}}{W_{in}} \quad (1)$$

The heat out (Q_{out}) was equated to the heat absorbed by the water in the tank, represented by the equation,

$$Q_{out} = \sum_{t=0}^{T} (\Delta\, Q_{water})_t \tag{2}$$

where,

$$\Delta Q_{water} = \sum_{k=1}^{6} m_k c_p \Delta T_k \tag{3}$$

Total energy input ($W_{electrical}$) was calculated by summing the power input for each time step change.

$$W_{in} = \sum_{t=0}^{T} W_{electrical} \tag{4}$$

3.2 Exergy Analysis Formulation

The exergy analysis used in this study provides exergy destruction values for each component and exergy efficiency for the cycle. This analysis was carried out based on the following assumptions. 1) All components are in steady-state conditions, 2) heat and pressure losses from the pipes are negligible, 3) there is only heat transfer between the refrigerant and fluids flowing through the evaporator and condenser, and 4) kinetic energy, potential energy and exergy losses are negligible. The aforementioned assumptions were made to facilitate the analysis of performance variations attributed to specific factors of interest, such as ambient temperature and refrigerant charge while disregarding the influence of pressure losses.

Based on the steady-state exergy rate balance for a single inlet and outlet system, the exergy destruction can be derived according to [23] as follows,

$$\dot{I} = \dot{m}(\psi_i - \psi_e) + \left(1 - \frac{T_0}{T_j}\right)\dot{Q}_j - \dot{W}_{cv} \tag{5}$$

where the specific exergy is given by,

$$\psi = (h - h_0) - T_0(s - s_0) \tag{6}$$

thus for each of the main components,
compressor:

$$\dot{I} = \dot{m}[(h_1 - h_2) - T_0(s_1 - s_2)] + \dot{W}_{el} \tag{7}$$

where,

$$\dot{W}_{el} = \frac{\dot{m}(h_2 - h_1)}{\eta_{mech} \times \eta_{el}} \tag{8}$$

condenser:

$$\dot{I} = \dot{m}[(h_2 - h_3) - T_0(s_2 - s_3)] + \left(1 - \frac{T_0}{T_{cond}}\right)\dot{Q}_{cond} \quad (9)$$

TX Valve:

$$\dot{I} = \dot{m}[T_0(s_4 - s_3)] \quad (10)$$

Evaporator:

$$\dot{I} = \dot{m}[(h_4 - h_1) - T_0(s_4 - s_1)] + \left(1 - \frac{T_0}{T_{evap}}\right)\dot{Q}_{evap} \quad (11)$$

The exergy efficiency for a HPWH is given by,

$$\eta_{ex} = \frac{\psi_2 - \psi_3}{W_{el}} \quad (12)$$

3.3 IMST-ART Simulation

IMST-ART can simulate a vapor-compression system by dividing the overall system into sub-models for the compressor, heat exchangers, expansion valve, accessories, and piping. This section provides an overview of the considerations implemented to model the physical system for the system's four main components. Table 5 shows the refrigerant properties for both R290 and R134a. The compressor was modeled by specifying the parameters listed in Table 6, and oil circulation was set at 1% to account for propane's high solubility. The Single Point Adjustment method was implemented by fitting the correlations through the specifications of a single point. As experimental data was available, input conditions, such as evaporation temperature, condensation temperature, sub-cooled and superheated temperatures, were prescribed.

Table 5 Refrigerant properties [24].

No.	Refrigerant	Boling Point @1 atm(K)	Freezing Point (K)	Critical Temp (K)	Critical Pr (bar)	ODP	GWP
HFC (Hydrofluorocarbons)							
R134a	Tetrafluroethane	247	176.55	374.25	40.67	0	1300
Hydrocarbons							
R290	Propane	231.07	85.49	369.83	42.1	0	3

Table 6 Input parameters to the compressor submodel.

Compressor Input Parameters	**Value**
Displacement	13.5 cm^3
Nominal Speed	2840 RPM
Nominal Power	650 W
Oil Volume	0.3 L

Oil Circulation Rate	1%

The brazed plate condenser was modelled by specifying the parameters in Table 7. Pressure drops across the condenser was not modelled as measured values were only approximately 10 kPa for R134a operation, and R290 operation was expected to be lower. These values are insignificant compared to the suction and discharge pressures which are in the order of 500 kPa and 2000 kPa, respectively. The condenser outlet condition was specified by the subcool values measured experimentally.

Table 7 Input parameters to the condenser submodel.

Condenser Input Parameters	**Value**
Heat Exchanger Type	Plate
No. of Plates	12
Secondary Fluid	Water
Inlet/Outlet Water Temperatures	44°C/60°C
Flow Arrangement	Counter-Current
Pump Power	30 W
Inlet Water Pressure	300 kPa

The TX valve was modelled in IMST-ART by assuming that the superheat can be maintained constant by the valve, given that the superheat was quite constant over the main working range of operating conditions. The model also assumes constant enthalpy across the valve, which was very close to the experimental conditions.

The evaporator tube and fin coil heat exchanger used in the test unit were modelled by specifying the parameters listed in Table 8. The inlet and outlet air temperatures were affected by the ambient test conditions, and were measured and prescribed as input parameters. Relative humidity values of 30%, 60%, 80% for ambient test temperatures were analyzed and specified as input parameters. The inlet air pressure was assumed to be slightly higher than the ambient air pressure, and a value of 101.3 kPa was used. As the details of the fan specifications were not available, an almost ideal static efficiency value was assumed.

Table 8 Input parameters to the evaporator submodel.

Evaporator Input Parameters	**Value**
Heat Exchanger Type	Coil
Secondary Fluid	Air
Inlet Air Temperature	Depends on ambient
Outlet Air Temperature	Depends on ambient
Relative Humidity	30%/60%/80%
Inlet Air Pressure	101.3 kPa
Static efficiency	95%

The modeling of the tube rows was important and carefully considered. In the actual system, the evaporator divided the three rows of 16 tubes into four circuits. Each of these circuits had an

inlet and outlet, representing four inlets and four outlets for the evaporator. The circuit pattern was recreated from drawing specifications and was modeled, as shown in Figure 5.

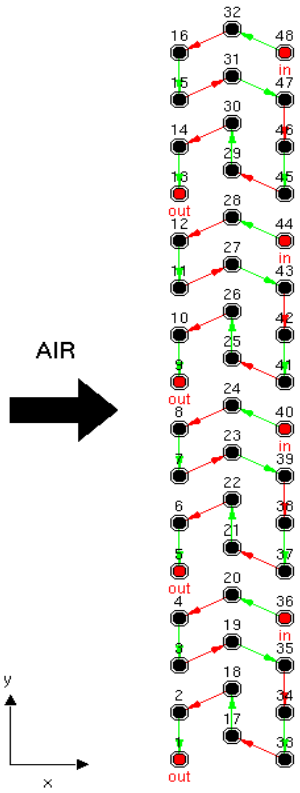

Figure 5 Evaporator circuit modelled with 4 circuits, staggered, 3 rows, 16 tubes per row.

4. Results and Discussions

4.1 COP and Heating Capacity

The COP values were determined from experimental measurements, and physical properties were extracted from thermocouple readings. The above data were used to calculate the volumetric flow rate ($\pm 10^{-3}$ m^3/s), specific heat capacity (±2 kJ/kg K), the temperature difference between the inlet and outlet temperatures of each component (±0.5°C), and total electrical energy consumption in the system (±20 W).

The COP values over ambient temperatures of 10, 15, 20, 25, 30°C for three charges of R290 (230 g, 260 g, 290 g) and one charge (700 g) of R134a were plotted together, as shown in Figure 6. It can be observed that at an ambient temperature of 10°C, the COP of R134a is consistently higher than R290 by 12% for all three charges. At an ambient temperature of 15°C, both R134a and all different charges of R290 exhibit equivalent COP values. However, at an ambient temperature of 20°C, although the 230 g and 290 g charges of R290 match the COP of R134a, the COP from the 260 g charge of R290 is 10% higher than R134a. Similarly, at an ambient temperature of 30°C, the 260 g charge of R290 resulted in 10% higher COP than R134a. The above results demonstrate an improvement in system performance when 260 g of R290 was used beyond 20°C ambient temperature. This indicates that the performance of R290 and R134a can

vary depending on the ambient temperature, with different charge levels of R290 achieving comparable or even superior COP values compared to R134a under certain conditions. Interestingly, a further increase in the charge of 290 g (from 260 g) of R290 decreased the system's performance. The exact reason for this is unclear and may be related to the fact that a charge of 290 g could have overcharged the system, raised the system operating pressure and temperature, and reduced the system's cooling ability. The ideal charge for this particular system is either at 260 g or very close to it at the ambient temperature beyond 14°C.

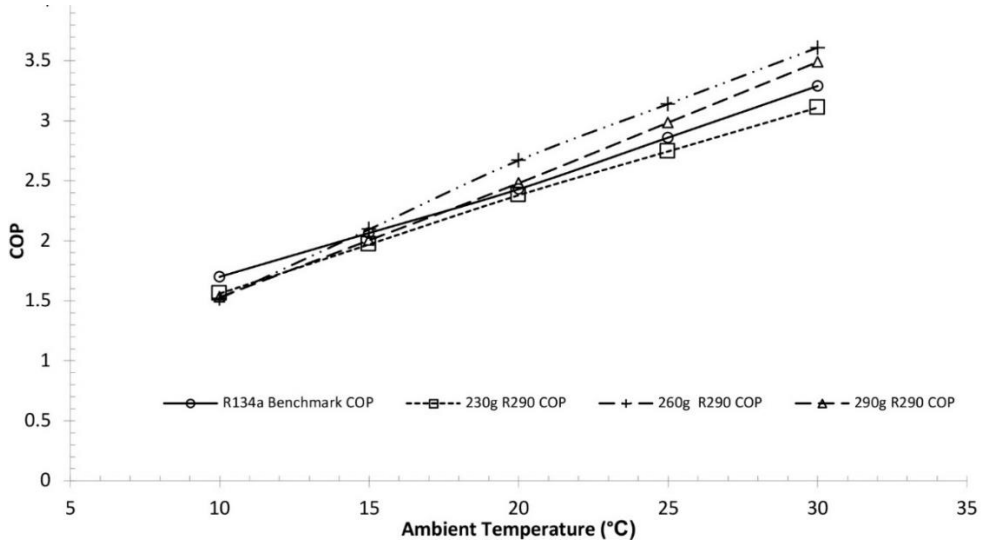

Figure 6 COP determined at five ambient temperatures for three charges of R290 and one charge of R134a.

A comparison was also made to the heating capacities of the tested charges in Figure 7. The 260 g charge of R290 was higher than the other configurations for heating capacity. Interestingly, all R290 charges possessed higher heating capacity than the 700 g charge of R134a. Lower COP was, however, observed for some of these configurations due to the higher power drawn.

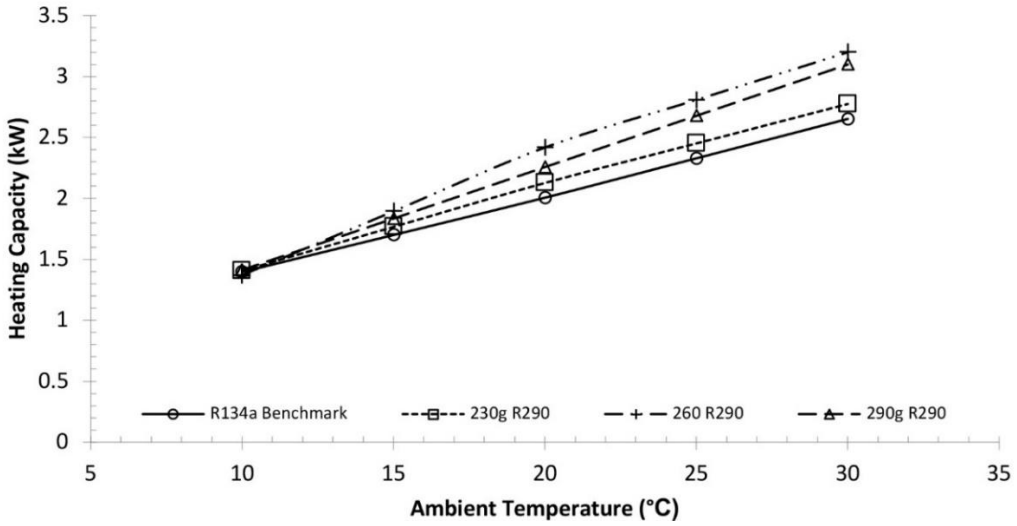

Figure 7 Heating capacity at five ambient temperatures for three charges of R290 and one charge of R134a.

4.2 Exergy Analysis Results

Exergy analysis was performed on experimental data for R290 under different ambient conditions and as a function of charges. Figure 8 illustrates that the compressor is responsible for the majority of exergy destruction, followed by the TX valve, with similar values for the condenser and evaporator. These findings are consistent with a previous study [18]. Furthermore, it can be observed that exergy destruction decreased with increasing evaporating temperature. This can be explained by the fact that a higher evaporating temperature means the temperature difference between the evaporator and its surroundings is smaller, resulting in lower exergy losses. However, it is worth noting that as the system possesses less exergy, it is closer to equilibrium with the environment. This trend aligns with the previous findings reported in [18-20].

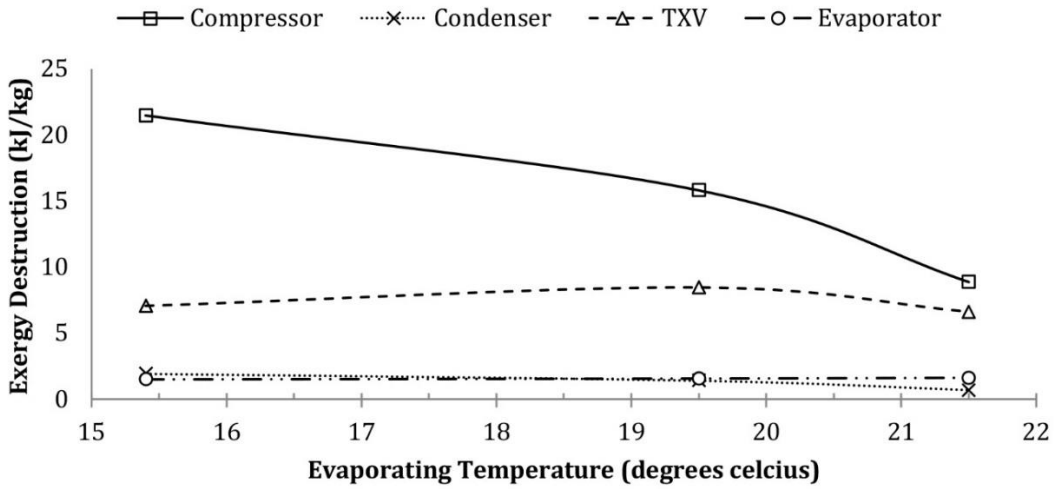

Figure 8 Variation of exergy destruction for each of the main components. Results are for R290 at 30°C ambient with a constant condensing temperature of 61°C.

Figure 9 displays the total exergy destruction and exergy efficiency for the entire HPWH system. The exergy efficiency increases with increasing evaporating temperature. Such observations are expected since exergy destruction indicates inefficiencies within the system, and exergy losses decrease with increasing evaporating temperature, as previously mentioned. Therefore, an increase in exergy efficiency can be expected. The exergy analysis performed in this work not only enables the quantification of exergy destruction but also its location in the HPWH by accounting for all exergy streams. This is highly beneficial as it helps determine the components/processes with the most significant irreversibility effects.

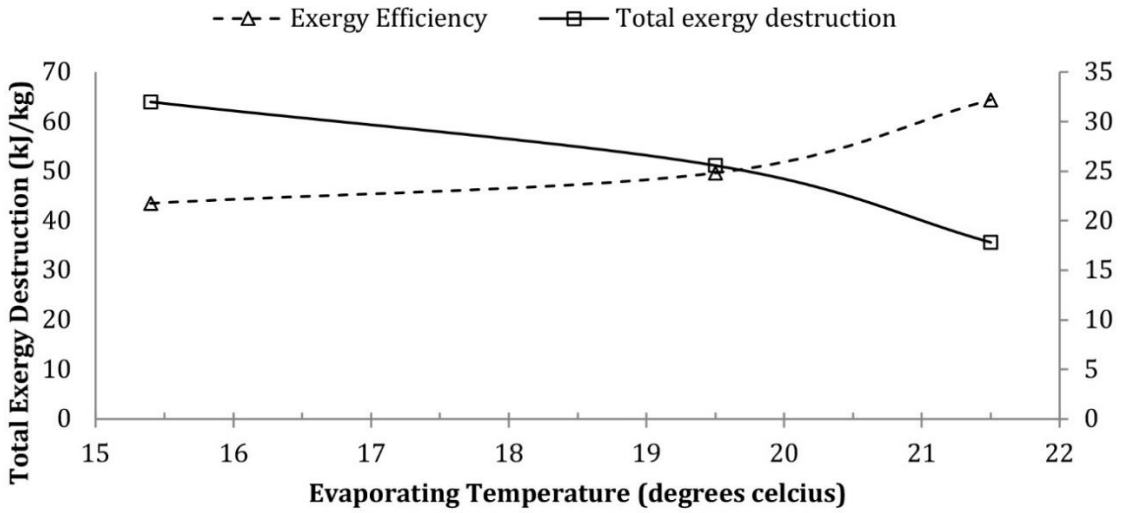

Figure 9 Total exergy destruction and Exergy efficiency for R290 at 30°C ambient with a constant condensing temperature of 61°C.

4.3 Simulation Results

The comparison between the simulated COP results and experimental results is a crucial step in validating the model. As shown in Figures 10 (a), (b), and (c), the experimental results for different R290 charges and ambient conditions were plotted along with the error bars defined as 15%, based on accepted practices and the specific characteristics of our experimental setup, as recommended by the manufacturer [22]. While the precision achieved during the experimental measurements may be subject to variations due to known sources of error, the chosen uncertainty value of 15% appropriately represents the level of confidence in the COP measurements obtained in this study. The results reveal that the model over-predicted the COP values for the 20°C, 25°C and 30°C ambient temperatures by 4-13%, 6-15% and 8-17%, respectively. However, for the 10°C ambient condition, the simulation consistently under-predicted the COP by 3%-15%. At the ambient temperature of 15°C, the discrepancy between simulation and experimental results are insignificant, i.e. 0%-7%. Despite the slight over-prediction at ambient temperature beyond 20°C, the predictions followed similar trends as the experimental results when analyzed as a function of temperature. It is worth noting that the model did not account for pressure losses across pipes and evaporators, which could explain the slight over-prediction observed. It is also important to mention that low relative error results in less than 5%, as achieved by [21], were not observed. Table 9 shows the percentage relative difference between the experimental and simulated COP results, indicating moderate correspondence at the over-predicted range of 4%-17% and under-predicted range of 3%-15%.

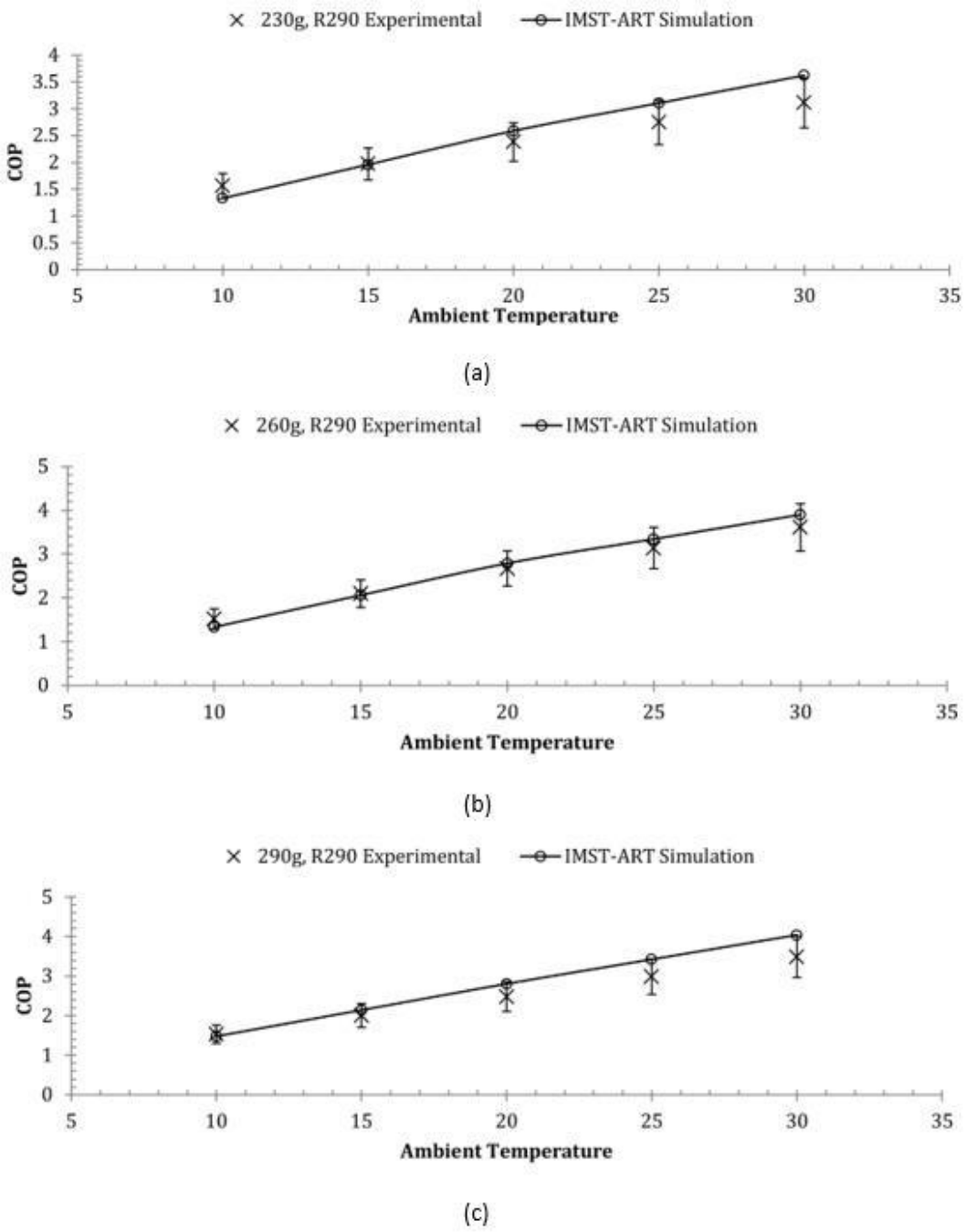

Figure 10 IMST-ART simulation for COP compared against experimental value for (a) 230 g charge of R290, (b) 260 g charge of R290 and (c) 290 g charge of R290.

Table 9 COP for experimental value and IMST-ART simulation at 230 g, 260 g and 290 g charge of R290.

Ambient Temperature	Experimental results	IMST-ART Simulation	% Relative Difference
	230 g, R290		
10	1.56	1.33	15%
15	1.97	1.96	1%
20	2.38	2.59	9%

25	2.75	3.1	13%
30	3.11	3.63	17%
		260 g, R290	
10	1.52	1.33	13%
15	2.1	2.1	0%
20	2.67	2.79	4%
25	3.14	3.34	6%
30	3.61	3.9	8%
		290 g, R290	
10	1.53	1.48	3%
15	2	2.14	7%
20	2.48	2.8	13%
25	2.99	3.42	15%
30	3.49	4.04	16%

Overall, while the model showed moderate correspondence with the experimental results, the discrepancies observed can provide valuable insights for future improvements. For instance, the under-prediction of COP at 10°C ambient condition suggests the need to optimize the system's performance at lower temperatures, perhaps through better insulation or the use of a different compressor. The over-prediction of COP at higher ambient temperatures could be attributed to the model's failure to account for pressure losses across pipes and evaporators. This highlights the importance of accurate modelling of the system's components and parameters to improve the model's accuracy. By identifying the model's limitations, new design suggestions could be potentially made for the HPWH system, leading to improved performance and energy efficiency.

With the model validated, new design suggestions can be explored to improve the performance of the HPWH system. One possibility is replacing the current compressor in the system with a compressor designed for use with R290. This idea was investigated through modelling in IMST-ART, where two new compressors were selected with similar displacement and power ratings to the compressor in the test unit. These compressors were the SIAM RE135VHSMT [25] and the SECOP SC12MNX [26]. Both compressors had a displacement of 12.87 cm^3, and their power consumption values were similar to the 650 W nominal value of the test unit compressor, although power consumption varies with load.

The SECOP compressor was particularly interesting as it was designed specifically for use with R290. Its compressor performance map could be used to model its performance in the established IMST-ART model. By keeping the same modelling parameters, the new SECOP compressor was tested based on the lowest, middle and highest ambient temperatures, i.e. 10, 20 and 30°C with a 260 g charge of R290. The results, shown in Figure 11, revealed that lower COP values were predicted with the new model for all ambient conditions. These findings suggest that replacing the compressor with one designed for use with R290 could improve the system's performance. It is worth noting, however, that further investigation and testing would be necessary to determine the feasibility and practicality of implementing such a change.

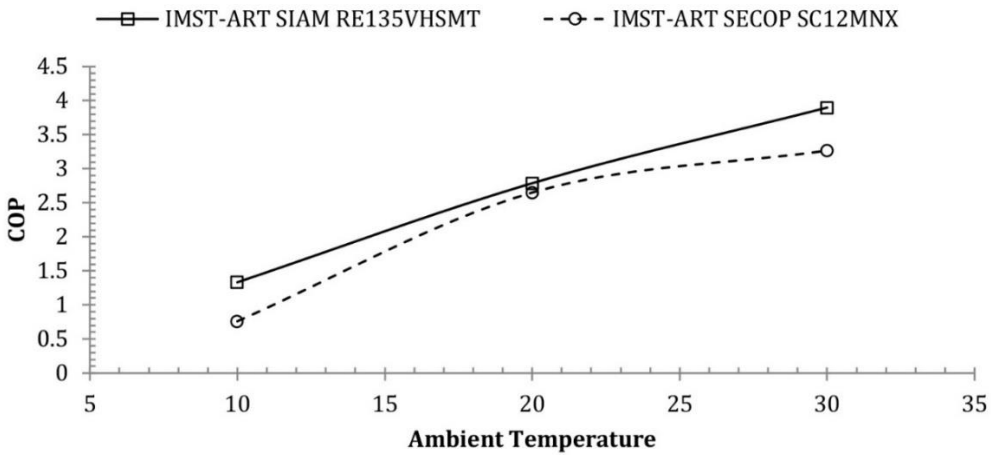

Figure 11 Comparing IMST-ART models with test unit compressor and SECOP R290 compressor.

There are a few possible reasons for the lower predicted performance of the SECOP compressor when compared to the original compressor. One potential factor is that the SECOP compressor is rated for the highest evaporating temperature of 10°C, while in the experiments, evaporating temperatures of 15°C were common at 20°C ambient temperature. At 30°C ambient temperature, the evaporating temperature was observed to be higher at around 20°C. This difference in operating conditions could have led to a lower predicted COP for the SECOP compressor.

Another factor that may have affected the predicted performance is that the refrigerant in the SECOP compressor is rated for a maximum charge of 150 g, whereas the prediction model used a charge of 260 g. This difference in refrigerant charge could have impacted the compressor's performance and contributed to the lower predicted COP. Despite these factors, it is worth noting that the SECOP compressor was designed and rated for R290 use, whereas the SIAM compressor was not. This is important from a practical standpoint, as uncertified compressors running on flammable refrigerants are unlikely to be put into production. Additionally, the low charge of R290 in the SECOP compressor is advantageous from the user's perspective, particularly in domestic settings, as long as heat exchangers can be sized correctly for their intended purpose.

Overall, the results of this investigation suggest that there is potential for improving the performance of HPWH systems through the use of compressors specifically designed for use with R290. While the SECOP compressor did not perform as well as expected in the prediction model, its use in production may still be viable given its certification for R290 use and low refrigerant charge.

5. Conclusions

This study aimed to investigate the performance of a HPWH system using R290 as a refrigerant under different ambient temperatures, and the results have implications for decarbonisation efforts across industries. The study used experimental and simulation methods to evaluate the system's performance and validate the simulation model, and the results showed moderate correspondence between the experimental and simulated results, with relative differences ranging from 4% to 17% for a common room temperature of 20°C to 30°C.

The study found that there was an over-prediction of COP values beyond the 20°C ambient temperatures, while the simulation consistently underpredicted the COP for the 10°C ambient condition. At an ambient temperature of 15°C, there is a strong concurrence between the simulation and experimental findings, demonstrating very good agreement between the two. Additionally, the study investigated the potential for improving the system's performance by using new compressors specifically designed for R290 use. The comparison between two new compressors showed that the SECOP compressor, which was designed and rated for R290 use, had lower predicted performance than the SIAM compressor, which was not designed for R290.

Furthermore, the results of this study have broader implications for decarbonisation efforts, particularly in the heating and cooling sector, which accounts for a significant portion of global carbon emissions. The use of HPWH systems, especially those using low-GWP refrigerants like R290, can play a crucial role in reducing carbon emissions and achieving decarbonisation goals. However, safety concerns related to flammable refrigerants like R290 must be considered, and the design and use of compressors for HPWH systems must ensure both performance and safety.

Future research in this area could further investigate the performance of HPWH systems using other low-GWP refrigerants and explore the potential for improving system efficiency through innovative design and technology. Overall, the findings of this study contribute to the growing body of knowledge on sustainable heating and cooling solutions and provide insights into the challenges and opportunities associated with decarbonisation efforts.

Nomenclature

g	gravitational force	(m/s^2)
μ	dynamic viscosity	($N.s)/m^2$
z	elevation	(m)
$\dot{I}$	exergy destruction rate	(-)
η_{ex}	exergy efficiency	(-)
$\dot{Q}$	heat transfer rate	(W)
$\dot{m}$	mass transfer rate	(kg/s)
$\dot{W}$	power	(W)
P	pressure	(Pa)
s	specific entropy	(J/kg.K)
ψ	specific exergy	(J/kg)
u	specific internal energy	(J/kg)
v	specific volume	(m^3/kg)
k	thermal conductivity	(W/m.K)
T	temperature	(°C)
V	velocity	(m/s)

Author Contributions

Conceptualization, A.L. and S.C.; methodology, A.L and S.C.; software, A.L.; investigation, A.L.; data curation, A.L.; writing—original draft preparation, A.L.; writing—review and editing, A.L and S.C.

Competing Interests

The authors have declared that no competing interests exist.

References

1. Hudon K, Sparn B, Christensen D, Maguire J. Heat pump water heater technology assessment based on laboratory research and energy simulation models. Proceeding of ASHRAE Winter Conference; 2012 January 21-25; Chicago, IL, USA.
2. Enrico DR, Davide DC. Performance of a semi-hermetic reciprocating compressor with propane and mineral oil. Int J Refrig. 2011; 34: 752-763.
3. Australian Government. HFC phase-down - Frequently asked questions [Internet]. Canberra, Australia: Australian Government-Department of Climate Change, Energy, the Environment and Water; 2021. Available from: http://www.environment.gov.au/protection/ozone/hfc-phase-down/hfc-phase-down-faqs.
4. Calm JM. The next generation of refrigerants - historical review, considerations, and outlook. Int J Refrig. 2008; 31: 1123-1133.
5. Björk E, Palm B. Performance of a domestic refrigerator under influence of varied expansion device capacity, refrigerant charge and ambient temperature. Int J Refrig. 2006; 29: 789-798.
6. Ciconkov R. Refrigerants: There is still no vision for sustainable solutions. Int J Refrig. 2018; 86: 441-448.
7. Aaron Leaman. Deadly Tamahere coolstore blaze: Remembering a day no one can forget [Internet]. Wellington, New Zealand: Stuff Digital; 2018. Available from: https://www.stuff.co.nz/business/industries/102402172/tamahere-coolstore-fire-remembering-a-day-no-one-can-forget.
8. New Zealand Fire Service Commission. Inquiry into the explosion and fire at Icepak Coolstores, Tamahere, on 5 April 2008 / New Zealand Fire Service. Wellington, New Zealand: New Zealand Fire Service Commission; 2008.
9. Dunse BL, Derek N, Fraser PJ, Krummel PB, Steel LP. Australian and global HFC, PFC, sulfur hexafluoride, nitrogen trifluoride and sulfuryl fluoride emissions. Report prepared for Australian Government Department of the Environment and Energy. Aspendale, Australia: CSIRO Oceans and Atmosphere; 2018. Available from: https://www.agriculture.gov.au/sites/default/files/documents/report-sgg.pdf.
10. Wicher A. Europe's Propane Refrigeration Proliferation. Emerson Climate Technologies. Available from: https://www.copeland.com/documents/v2-n3-feature-%E2%80%93-europe%E2%80%99s-propane-refrigeration-proliferation-en-ca-5438748.pdf.
11. Devotta S, Padalkar AS, Sane NK. Performance assessment of HC-290 as a drop-in substitute to HCFC-22 in a window air conditioner. Int J Refrig. 2005; 28: 594-604.
12. Maclaine-Cross IL, Leonardi E. Why hydrocarbons save energy. AIRAH J. 1997; 51: 33-38.
13. Secop GmbH. Practical application of refrigerant R600a and R290 in small hermetic systems [Internet]. Available from: https://www.secop.com/fileadmin/user_upload/technical-literature/guidelines/application_guideline_r600a_r290_02-2018_desa610a202.pdf.
14. Corberán JM, Martínez IO, Gonzálvez J. Charge optimisation study of a reversible water-to-water propane heat pump. Int J Refrig. 2008; 31: 716-726.

15. Corberán JM, Martínez-Galván I, Martínez-Ballester S, Gonzálvez-Maciá J, Royo-Pastor R. Influence of the source and sink temperatures on the optimal refrigerant charge of a water-to-water heat pump. Int J Refrig. 2011; 34: 881-892.
16. Fernando P, Palm B, Lundqvist P, Granryd E. Propane heat pump with low refrigerant charge: Design and laboratory tests. Int J Refrig. 2004; 27: 761-773.
17. Subramanian AS, Gundersen T, Adams TA. Modeling and simulation of energy systems: A review. Processes. 2018; 6: 238.
18. Ahamed JU, Saidur R, Masjuki HH, Sattar MA. An analysis of energy, exergy, and sustainable development of a vapor compression refrigeration system using hydrocarbon. Int J Green Energy. 2012; 9: 702-717.
19. Bayrakçi HC, Özgür AE. Energy and exergy analysis of vapor compression refrigeration system using pure hydrocarbon refrigerants. Int J Energy Res. 2009; 33: 1070-1075.
20. Anand S, Tyagi SK. Exergy analysis and experimental study of a vapor compression refrigeration cycle: A technical note. J Therm Anal Calorim. 2012; 110: 961-971.
21. Castro JB, Urchueguia JF, Corberan JM, Gonzálvez J. Optimized design of a heat exchanger for an air-to-water reversible heat pump working with propane (R290) as refrigerant: Modelling analysis and experimental observations. Appl Therm Eng. 2005; 25: 2450-2462.
22. Rheem. Rheem heat pump hot water [Internet]. Rydalmere, NSW, Australia; 2003. Available from: https://www.sahotwater.com.au/specifications/Rheem_Heat_Pump_System_Brochure.pdf.
23. Cengel YA, Boles MA, Kanoğlu M. Thermodynamics: An engineering approach. New York: McGraw-hill; 2011.
24. Venkatarathnam G, Srinivasa Murthy S. Refrigerants for vapour compression refrigeration systems. Resonance. 2012; 17: 139-162.
25. Siam Compressor Industry Co., Ltd. The most advanced compressor technology for environment consciousness [Internet]. Bangkok, Thailand: Siam Compressor Industry Co., Ltd.; 2023. Available from: https://siamcompressor.com/index.php/files/download/3b8580d0bb83839.
26. Secop. SC12MNX MBP Compressor R290 220-240V 50Hz [Internet]. Flensburg, Germany: Secop GmbH; 2018. Available from: https://www.secop.com/fileadmin/user_upload/SEPS/datasheets/sc12mnx_104h8275_r290_220v_50hz_10-2018_desd560u302.pdf.